

# Defect-Assisted Heteroepitaxial Growth of Monolayer Tungsten Diselenide Films with Preferential Orientation on Hexagonal Boron Nitride

**Xiaotian Zhang<sup>1</sup>, Fu Zhang<sup>1,3</sup>, Yuanxi Wang<sup>2,3</sup>, Daniel S. Schulman<sup>1</sup>, Tianyi Zhang<sup>1,3</sup>, Anushka Bansal<sup>1</sup>, Nasim Alem<sup>1,2</sup>, Saptarshi Das<sup>4</sup>, Vincent H. Crespi<sup>2,5</sup>, Mauricio Terrones<sup>3,5</sup>, and Joan M. Redwing<sup>1,2</sup>**

*Department of Materials Science and Engineering, The Pennsylvania State University, University Park, PA, 16802, USA*

*<sup>2</sup>2D Crystal Consortium, The Pennsylvania State University, University Park, PA, 16802, USA*

*<sup>3</sup>Center for Two Dimensional and Layered Materials, The Pennsylvania State University, University Park, PA 16802, USA*

*<sup>4</sup>Department of Engineering Science and Mechanics, The Pennsylvania State University, University Park, PA 16802, USA*

*<sup>5</sup>Department of Physics, The Pennsylvania State University, University Park, PA 16802, USA*

The rapid development of device technologies based on 2D transition metal dichalcogenides (TMDs) causes increasing demand for synthesis of high quality large area monolayer and few layer films. Our previous work demonstrated epitaxial growth of large area monolayer WSe<sub>2</sub> films on c-plane sapphire using gas source chemical vapor deposition (CVD). However, the optical and electrical properties of coalesced monolayer films grown on sapphire are negatively impacted by the existence of anti-phase boundaries (APBs) as well as non-uniformities arising from steps and charge-induced doping associated with the sapphire surface. Prior studies demonstrated a preferred domain orientation for TMDs grown on hBN and first-principle calculations suggest this phenomenon originates from single atom vacancies on the hBN surface that act as nucleation sites. In this study, we further investigate the mechanism of defect-assisted domain alignment of 2D TMDs on hBN and demonstrate the growth of fully-coalesced WSe<sub>2</sub> films on hBN with a reduced density of APBs and improved optical and electrical properties compared to films grown on sapphire.

WSe<sub>2</sub> monolayer films were grown by gas source CVD at 800°C using W(CO)<sub>6</sub> and H<sub>2</sub>Se in a H<sub>2</sub> carrier gas employing a multi-step process to separately control nucleation density and lateral growth and coalescence of domains. Single crystal hBN flakes exfoliated from bulk crystals and transferred onto c-plane sapphire were used as substrates. He plasma treatment and NH<sub>3</sub> annealing were used to modify the surface defect density of hBN. Detailed studies of WSe<sub>2</sub> deposition on hBN as a function of growth conditions and substrate pre-treatment confirm that domain nucleation is controlled by the surface defect density rather than the precursor concentration. Over 90% of WSe<sub>2</sub> domains have consistent orientation via the defect-assisted growth. Through careful control of nucleation and extended lateral growth time, fully coalesced WSe<sub>2</sub> monolayer films on hBN were produced for subsequent characterization. High resolution scanning transmission electron microscopy (S/TEM) analysis demonstrates the absence of APBs in coalesced regions formed by the merging of 0° oriented domains. Temperature-dependent photoluminescence measurements show sharp and enhanced exciton and trion emission peaks, with no defect-related bound exciton emission from monolayer WSe<sub>2</sub>/hBN down to 80K. Backgated FET devices fabricated on WSe<sub>2</sub>/hBN films transferred to SiO<sub>2</sub>/Si substrates show an order of magnitude increase in room temperature carrier mobility (~5 cm<sup>2</sup>/V-s) compared to similar devices fabricated using monolayer WSe<sub>2</sub> films transferred from sapphire.

## Supplementary Pages

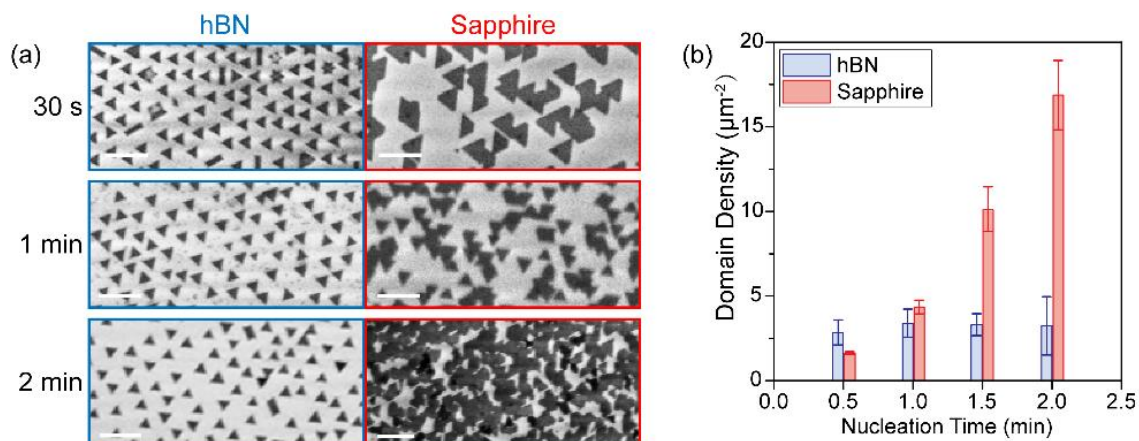


**Figure 1.** (a) SEM images of WSe<sub>2</sub> domains grown on hBN (left) and sapphire (right) respectively under varied nucleation time of 30s, 1 min, and 2min. Scale bar: 1 μm. (b) Domain density histogram versus nucleation time showing the nucleation on hBN is not controlled by the amount of precursors on the surface.

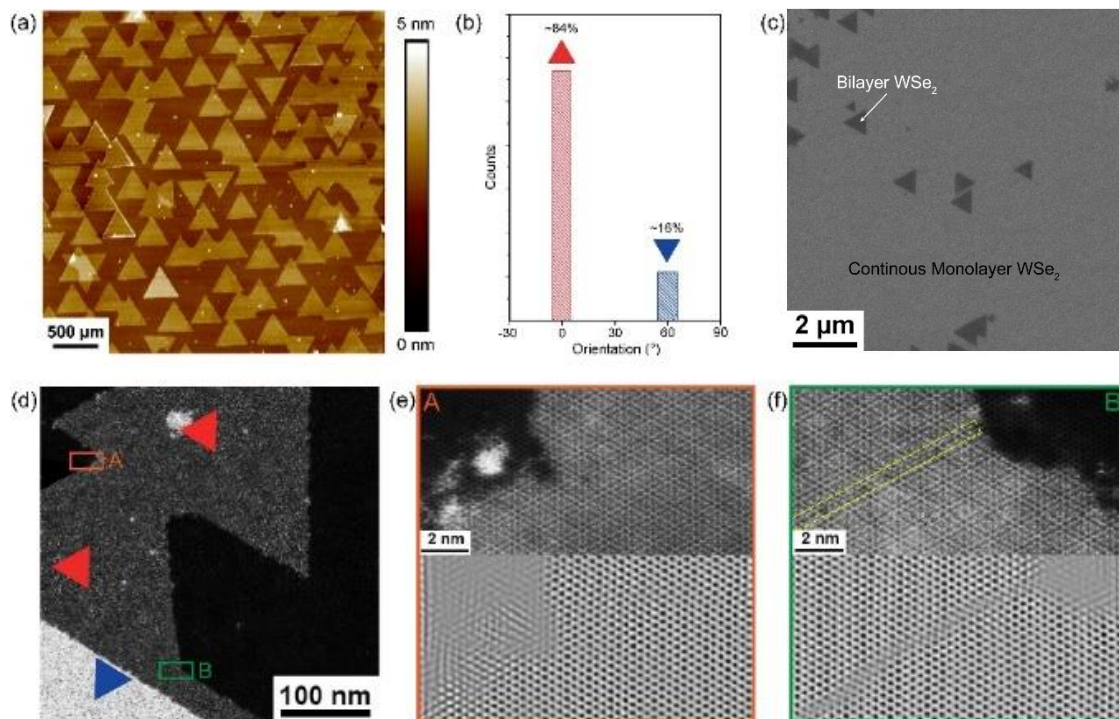


**Figure 2.** (a) AFM image of epitaxial WSe<sub>2</sub> domains on hBN. (b) Orientation histogram of 0° and 180° oriented WSe domains on hBN. (c) SEM image of coalesced monolayer WSe<sub>2</sub> film on hBN. (d) ADF-STEM image of region with two types of merging domains. (e) HAADF-STEM image of region A in (d) showing no grain boundary formed between 0° and 180° domains with same orientation. (f) HAADF-STEM image of region B in (d) showing mirror grain boundary formed between two domains with orientation.

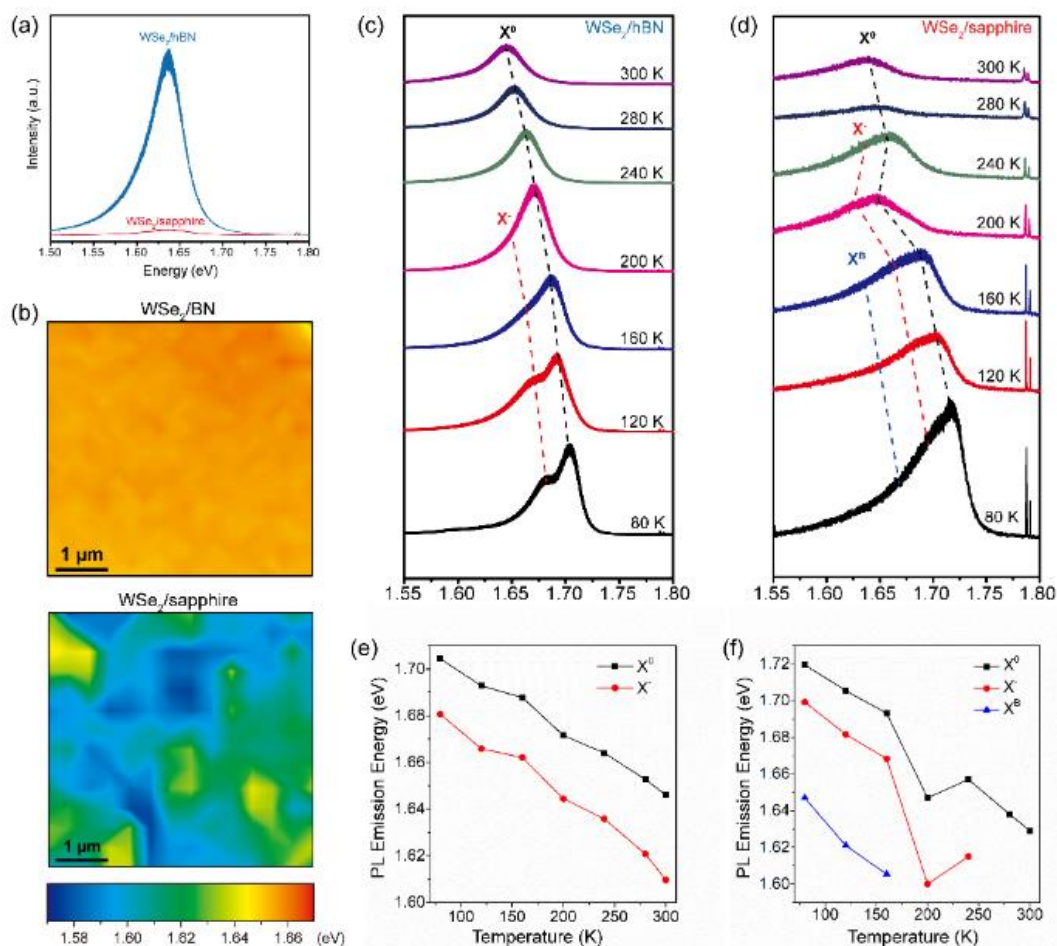


**Figure 3.** (a) PL spectra and (b) PL peak position maps of WSe<sub>2</sub> on hBN (blue, top) and sapphire (red, bottom). (c)-(d) Temperature-dependent PL spectra of WSe<sub>2</sub> on hBN and sapphire under 488 nm laser excitation, respectively. (e)-(f) PL emission peak energy of WSe<sub>2</sub> on hBN and sapphire versus temperature.

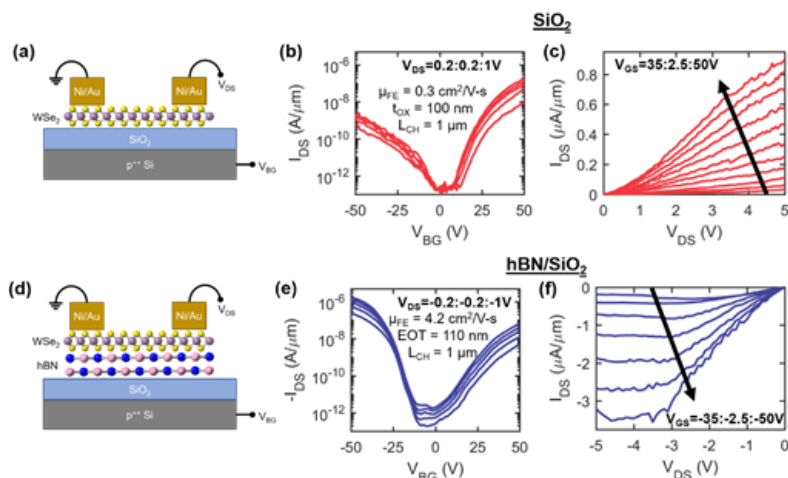


**Figure 4.** Electrical FET characterization of WSe<sub>2</sub> on SiO<sub>2</sub> and hBN/SiO<sub>2</sub>. Schematic showing a back gated WSe<sub>2</sub> FETs (a) directly on 100 nm SiO<sub>2</sub> and (d) on 10 nm hBN on 100 nm SiO<sub>2</sub> on p<sup>++</sup> Si with Ni contacts. (b,e) Drain current ( $I_{DS}$ ) versus back gate voltage ( $V_{BG}$ ) at various drain voltages ( $V_{DS}$ ) and (c,f)  $I_{DS}$  versus  $V_{DS}$  at various  $V_{BG}$  for WSe<sub>2</sub> on SiO<sub>2</sub> and on hBN/SiO<sub>2</sub>, respectively.